Archives of Acoustics Vol. 50, No. 4, pp. 421–433 (2025), https://doi.org/10.24425/aoa.2025.154831

Research Paper

Comparison of Methods for Determining the Airflow Resistivity of Porous and Covering Materials

Mykhaylo MELNYK[(1)], Jarosław RUBACHA[(2)*], Artur FLACH[(2)], Aleksandra CHOJAK[(2)], Tadeusz KAMISIŃSKI[(2)], Wojciech ZABIEROWSKI[(3)], Marek IWANIEC[(4)], Andriy KERNYTSKYY[(1)]

[(1)] *Department of Computer Aided Design Systems, Lviv Polytechnic National University*
Lviv, Ukraine

[(2)] *Department of Mechanics and Vibroacoustics, Faculty of Mechanical Engineering and Robotics, AGH University of Krakow*
Krakow, Poland

[(3)] *Department of Microelectronics and Computer Science, Lodz University of Technology*
Łódź, Poland

[(4)] *Department of Biocybernetics and Biomedical Engineering, Faculty of Electrical Engineering, Automatics, Computer Science and Biomedical Engineering, AGH University of Krakow*
Krakow, Poland

*Corresponding Author e-mail: jrubacha@agh.edu.pl

Received July 15, 2024; revised March 21, 2025; accepted September 21, 2025; published online November 13, 2025.

This article compares two methods for determining the airflow resistivity of porous and coating materials – a key parameter in sound absorption modelling. The analysis involves a modified static airflow measurement procedure in accordance with International Organization for Standardization [ISO] (2018), using a linear approximation algorithm (PLA), and a reverse method consisting of matching the measured absorption coefficient in an impedance tube to the Miki model. The analysis was conducted on both porous materials utilised in acoustic panel fillings and thin coverings. It is evident that both methods yield analogous outcomes for materials exhibiting low resistivity. However, for materials characterised by higher resistivity, discrepancies of up to 50 % were observed. Nevertheless, a high degree of agreement was obtained between the calculated and measured absorption coefficients. For thin coating materials, an air gap of at least 70 mm is required. For materials with a thickness of up to approximately 30 mm, differences in resistivity do not significantly affect the absorption coefficient. It is evident that both methods can be used to determine the airflow resistivity of porous materials and layered structures, supporting the effective selection of materials according to requirements.

Keywords: airflow resistivity; specific airflow resistance; sound absorption coefficient; impedance tube; porous materials.

1. Introduction

Porous media are used in various practical applications such as sound absorption and noise control (Allard, Atalla, 2009; Gibson, Ashby, 1997; Tao *et al.*, 2021). Porous structures present exceptional sound-absorbing properties in the mid-to-high-frequency ranges (Cao *et al.*, 2018; Zhao *et al.*, 2016). Porous materials are mesh-like structures with interconnected pores (Oliva, Hongisto, 2013). The pro-

cesses inside the pores, associated with the fluid's viscosity, generate heat from sound energy (Crocker, 2007; Huang *et al.*, 2023). Porous structures can be organic, inorganic, or mixed composite materials, including stone, wood, sponge, foam, rubber, non-woven fabrics, and textiles (Doutres *et al.*, 2010; Johnson *et al.*, 1987; Lafarge *et al.*, 1997).

The basic parameter describing the sound-absorbing properties of a material is its sound absorption coefficient a, defined as the part of incident energy that is not reflected (Allard, Atalla, 2009):

$$a = 1 - \frac{E_r}{E_{\text{tot}}}, \tag{1}$$

where E_r and E_{tot} are the acoustic energies of the reflected and incident waves, respectively.

The sound absorption coefficient can be determined by measurements in an impedance tube, using either the standing wave method (ISO, 1996) or the transfer function method (ISO, 2023). Measurements in the impedance tube are characterized by very good accuracy, cost-effectiveness, and testing flexibility. The sound absorption coefficient can also be established in a reverberation room (ISO, 2003; Vorländer, 2008). This procedure allows for the measurement of both flat and spatial elements, including auditorium chairs (Cuenca *et al.*, 2022; Rubacha *et al.*, 2012). However, this technique requires the use of specialized reverberation rooms. As an alternative to physical measurements, the sound absorption coefficient can also be determined using empirical models. These models are based on a large number of measurements of different materials, and the interpretation of the physical processes occurring in these materials. Delany and Bazley (1970), and later Miki (1990) proposed the simplest empirical models, which require only one parameter: airflow resistivity. Johnson *et al.* (1987), as well as Allard and Champoux (1992), suggested a more accurate physical model (the Johnson–Champoux–Allard (JCA) model) with five input parameters. Unfortunately, these parameters are usually difficult to estimate accurately. Bonfiglio and Pompoli (2013) presented an inverse method for determining the physical parameters of porous materials for use with the JCA model. Also, Vorländer (2008) discussed the difficulties in determining the parameters of porous media due to the complexity and variability of these materials, including factors such as geometrical configuration, porosity, and tortuosity for the JCA model. This means that more complex models may give worse results, with errors that are difficult to estimate.

Airflow resistivity is one of the basic parameters describing porous and nonwoven materials. It is used as input parameter for models, enabling the calculation of the sound absorption coefficient of single- and multi-layer materials using the transfer matrix method (Cox, D'Antonio, 2016; Dell *et al.*, 2021; Herrero-Durá *et al.*, 2019; Hou *et al.*, 2017). Kamisiński *et al.* (2012) showed that it can also be used to calculate the sound absorption coefficient of materials with coverings. The measurement of airflow resistivity is conducted according to two standards: ASTM C522-03 (2022) and ISO 9053-1 (2018). The primary distinctions between these two standards pertain to the measurement conditions specified for assessing airflow resistivity. ASTM C522-03 allows measurements in flow directions other than perpendicular, provided the airflow remains constant. On the other hand, ISO 9053-1 allows variable airflow measurements, but solely for flow that is perpendicular to the sample.

Both standards mandate measurements to be conducted under laminar flow conditions, ensuring the airflow resistance remains constant as flow speed varies. The ISO standard specifies that airflow resistance should be determined at a flow speed of $0.5 \cdot 10^{-3}$ m/s, either directly or by extrapolation from higher values if direct measurement is unfeasible at such a low velocities. Meanwhile, the ASTM standard mandates measurements at three different laminar flow rates, each differing by at least 25 %.

Melnyk *et al.* (2018) proposed a modification to the standardized method of measuring airflow resistivity. They suggested using the previous linear approximation method (PLA) method to improve the accuracy of the technique for measuring airflow resistance under static airflow conditions. Moreover, they analyzed an inverse method for determining airflow resistivity based on fitting sound absorption coefficients.

Similarly, Sebaa *et al.* (2005) proposed a method for determining the airflow resistivity of porous materials by analyzing the reflection of a plane wave from the porous material. The described method involves fitting the measured impulse reflected from the tested material to an impulse calculated with a time-domain model. The model, developed by Johnson *et al.* (1987), integrates porosity and airflow resistivity and was used in the computations. Sensitivity analysis showed that sound reflection is most sensitive to airflow resistivity, while the influence of porosity is minimal. Jeong (2020) also presented a parallel technique for estimating airflow resistivity. However, his method was based on fitting the measurements of the sound absorption coefficient acquired in a reverberation chamber. Currently, machine learning (ML) techniques are widely used in the inverse method to characterize porous acoustic materials (Müller-Giebeler *et al.*, 2024; Zea *et al.*, 2023).

This paper aims to compare two methods used to estimate airflow resistivity. The first one is a modified standardized method that calculates static airflow through a porous material. The second method is an inverse method, based on fitting the sound absorption coefficient calculated from the airflow resistivity to the values measured in an impedance tube. The paper also

includes an extension of the inverse method for determining airflow resistivity in thin upholstery materials. The obtained results allow for an analysis of the accuracy of the investigated methods for determining airflow resistivity across different types of materials.

2. Methods for determining airflow resistivity

2.1. Standardized method – static airflow method

The standardized method for testing the airflow resistivity of porous materials, as outlined in (ASTM, 2022; ISO, 2018), is based on static airflow. This method involves the control of the airflow through the sample under examination while simultaneously measuring the pressure before and after the sample. The measurement should be conducted with airflow velocities ranging from $5 \cdot 10^{-4}$ m/s to $4 \cdot 10^{-3}$ m/s (ASTM, 2022) or 50 mm/s (ISO, 2018). By recording the sound pressure drop Δp and the volumetric airflow rate q_v, it is possible to calculate the airflow resistance R:

$$R = \frac{\Delta p}{q_v}. \tag{2}$$

Then, the specific airflow resistance (R_s) is determined, a parameter independent of the area of the sample:

$$R_s = R \cdot A = \frac{\Delta p}{q_v} \cdot A = \frac{\Delta p}{Au} \cdot A = \frac{\Delta p}{u}, \tag{3}$$

where $u = q_v/A$ is the airflow velocity, and A is the area of the sample perpendicular to the airflow.

Finally, a parameter independent of the thickness of the sample – the airflow resistivity r_s is determined:

$$r_s = \frac{R_s}{D}, \tag{4}$$

where D is the thickness of the material.

The standard method for measuring the pressure drop involves the use of the smallest possible value of airflow velocity, $u = 5 \cdot 10^{-4}$ m/s. An alternative approach involves a gradual reduction of the airflow velocity. In this approach, the relationship between airflow resistance and airflow velocity is determined for each sample using linear regression $R_s(u)$, and the final value of R_s is taken at $5 \cdot 10^{-4}$ m/s.

2.2. Modification of the standardized method

Melnyk *et al.* (2018) conducted a study that proposed modifications to the airflow resistivity measurement method described in ISO (2018). Their research demonstrated that at low airflow velocities u, there is a significant nonlinearity in the relationship between the airflow resistance R_s and airflow velocity u (see Fig. 1). As a result, applying linear regression for extrapolation at low airflow velocities can lead to substantial errors. To circumvent this issue, a modification to the static airflow method was proposed, called the PLA iteration method. This method involves first the determination of a polynomial that describes the relationship between airflow velocity and pressure drop $q(\Delta p)$, followed by the transformation of this polynomial into a linear approximation of airflow resistance as a function of airflow velocity. The process commences at the highest airflow velocity, and in each iteration, the range is extended to include lower airflow velocity values. The error between the measured results and the linear regression model is calculated at each iteration, and iterations continue until the error does not exceed a predefined value. Finally, the determined polynomial is extrapolated to obtain the airflow resistance value at $u = 5 \cdot 10^{-4}$ m/s.

Figure 1 illustrates the relationship between airflow resistance and the linear velocity of a porous material, as determined in the experiment. The graph also

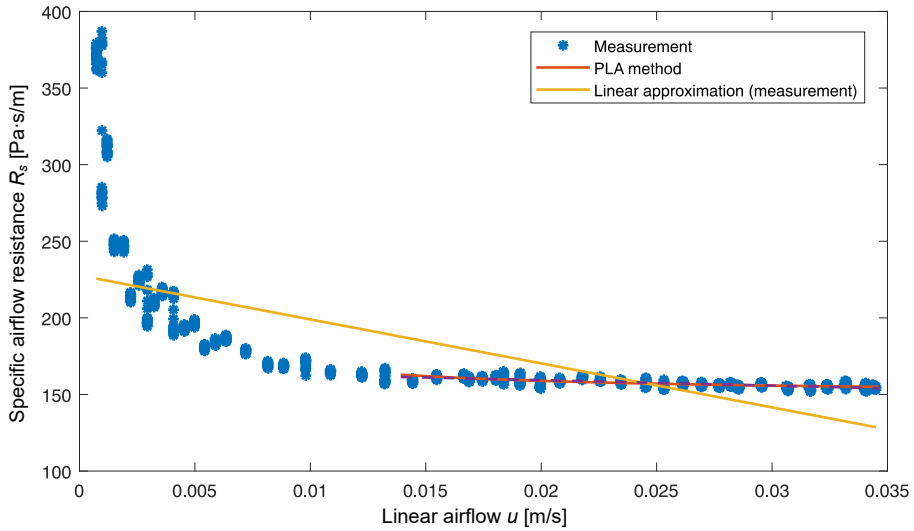

Fig. 1. Airflow resistance R_s of a porous material as determined in the measurement and a comparison of the regression line determined for the entire measurement range with the proposed PLA interpolation method.

presents regression lines calculated for the entire set of measurement data (yellow line), as well as for the data sets restricted by the proposed PLA method (red line).

The proposed PLA interpolation method, improves the alignment of the regression line with the measurement data in comparison to the linear approximation over the entire range of linear velocities u. This method effectively identifies the range of linear relationship between airflow resistance and airflow velocity by eliminating outliers. Consequently, it enhances the accuracy of airflow resistance determinations.

To automate the process of measuring airflow resistance, the laboratory setup (Fig. 2) uses sensors that are compatible with data acquisition cards. The measurement procedure involves the following steps: first, the test sample is mounted inside a cylinder. Air is then passed through the sample while simultaneously recording both the airflow rate and the pressure difference across the sample. For each test sample, a graph is created to illustrate the relationship between pressure and airflow. Finally, the airflow resistance at a linear velocity $u = 5 \cdot 10^{-4}$ m/s is determined using the PLA method.

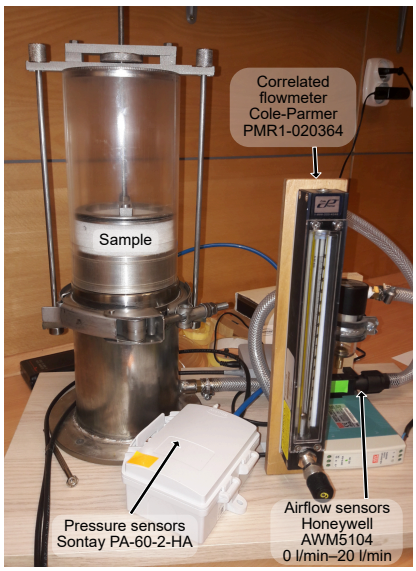

Fig. 2. Laboratory stand for determining the airflow resistivity of porous materials.

2.3. Inverse method for determining the airflow resistivity of porous materials

The proposed inverse method involves determining the flow resistivity through fitting the theoretical sound absorption coefficient to the measured value. To estimate the theoretical sound absorption coefficient, the Miki empirical model (Miki, 1990) was employed, which is a modification of the Delany–Bazley model (Delany, Bazley, 1970). The empirical model is based on experimental results and is a simplified description of the complex acoustic phenomena that occur in porous materials. It describes the relationship between key acoustic parameters of porous materials, such as characteristic impedance and propagation constant, and the physical parameter of airflow resistivity. The accuracy of the model is limited by the range of experimental data from which it was developed.

This model requires only a single parameter: the flow resistivity of the porous material. The model assumes that the solid phase is perfectly rigid and only considers the motion of the fluid. It is applicable to fibrous porous media with a porosity close to unity and provides the best fit to the experimental data in the range $0.01 < (f/r_s) < 1$. These models enable the prediction of the acoustic properties of porous materials, including specific impedance (z_c) and propagation constant (k_c).

In order to solve the inverse problem, it is necessary to find the minimum of the cost function $U(r_s)$, which is defined as follows:

$$U(r_s) = \sqrt{\frac{\sum_{i=1}^{n} \left(\alpha_t(f_i, r_s) - a_m(f_i)\right)^2}{N}}, \tag{5}$$

where $\alpha_t(f_i, r_s)$ is the predicted sound absorption coefficient for the i-th frequency band and for a given airflow resistivity r_s; $a_m(f_i)$ is the experimental sound absorption coefficient for the i-th frequency band, and N is the number of frequency bands. The bisection method is used to find the minimum of the cost function $U(r_s)$. By subdividing the initial interval into ten subintervals, calculations are accelerated, leading to faster results. The algorithm is fully detailed in the comprehensive study by Melnyk *et al.* (2018).

According to Miki's model, the propagation of sound in an isotropic, homogenous material is determined by two complex quantities:

– the characteristic impedance:

$$z_c(f) = \rho_0 c_0 \left[R(f) + jX(f)\right], \tag{6}$$

– the propagation constant (wavenumber) $k_c(f)$:

$$k_c(f) = \alpha + j\beta. \tag{7}$$

Based on the airflow resistivity r_s for a given material, the characteristic quantities can be determined using:

$$R(f) = \rho_0 c_0 \left[1 + 0.070 \left(\frac{f}{r_s}\right)^{-0.632}\right], \tag{8}$$

$$X(f) = \rho_0 c_0 \left[-0.107 \left(\frac{f}{r_s}\right)^{-0.632}\right], \tag{9}$$

$$\alpha = \frac{\omega}{c_0} \left[1 + 0.109 \left(\frac{f}{r_s}\right)^{-0.618}\right], \tag{10}$$

$$\beta = \frac{\omega}{c_0} \left[0.160 \left(\frac{f}{r_s}\right)^{-0.618}\right], \tag{11}$$

where $\omega = 2\pi f$, f is the frequency, ρ_0 is the air density, c_0 is the sound speed in air, and r_s is the airflow resistivity. Equations (8)–(11) were derived from regression models fitted to the relationship between the real parts $R(f)$ and $a(f)$, and the imaginary parts $X(f)$ and $b(f)$, of the acoustic impedance and propagation constant, respectively, with respect to the normalised flow resistance – expressed as (f/r_s) (Miki, 1990). The values for flow resistivity, acoustic impedance, and propagation constant were determined from measurements conducted on different materials (Delany, Bazley, 1970).

The surface impedance is then determined by

$$z_w = -i \cdot z_c \cdot \cot(kc \cdot D), \tag{12}$$

where D is the thickness of the material.

The formula to calculate the sound reflection coefficient R is

$$R = \frac{\frac{z_w}{\rho_0 c_0}\cos(\theta) - 1}{\frac{z_w}{\rho_0 c_0}\cos(\theta) + 1}, \tag{13}$$

where θ is the incidence angle, and for normal incidence $\theta = 0$.

The formula for the sound absorption coefficient $a_{t,i}$ is

$$\alpha_{t,i} = 1 - \left|R^2\right|. \tag{14}$$

2.4. Inverse method for determining the airflow resistivity of covering materials

The inverse method has also been used to calculate the airflow resistivity of covering materials. Similar to porous materials, a numerical model is required to find the sound absorption coefficient. For porous materials, it was assumed that the sound absorption coefficient can be determined for a model of the covering material placed on an air gap with a thickness of D. Therefore, the model describing the acoustic impedance of the surface of the material z_w, placed at a distance, was used to determine the sound absorption coefficient:

$$z_w = \frac{-j z_{s0} z_c \cot(k_c L) + z_c^2}{z_{s0} - j z_c \cot(k_c L)}, \tag{15}$$

where $z_{s0} = -j z_0 \cot(k_0 L)$ is the surface impedance at the top of the air layer of thickness L behind the material, $z_0 = \rho_0 c_0$ is the acoustic impedance of air, k_0 is the wave number in air, and z_c, k_c are the characteristic impedance and wave number of the covering material, respectively. Then, using Eqs. (13) and (14), the reflection coefficient R and sound absorption coefficient $a_{t,i}$ were calculated. The values of airflow resistivity were determined by the inverse method by finding the minimum of the cost function.

2.5. Sensitivity analysis of the porous material models

A sensitivity analysis was conducted for both the porous material model and the covering model where the covering material is mounted with an air gap behind, to investigate their applicability for the inverse method. The sensitivity of the models to changes in airflow resistivity was investigated. To evaluate the sensitivity of the models, the sensitivity index S_i was determined using the following relationship (Saltelli *et al.*, 2004):

$$S_i = \frac{\partial \alpha_i}{\partial r_s}\frac{r_s}{\alpha_i}, \tag{16}$$

where the differential $\frac{\partial \alpha_i}{\partial r_s}$ was calculated numerically for the sound absorption coefficient a_i at the i-th frequency for a given airflow resistivity r_s. The index provides a non-dimensional measure of sensitivity, showing how much the sound absorption coefficient is affected by a unit change in airflow resistivity. A higher S_i value indicates greater sensitivity, meaning that small variations in airflow resistivity lead to significant changes in the sound absorption properties of the material.

The analysis of porous materials was performed for materials with:

- low airflow resistivity ($r_s = 5000\,\mathrm{Pa\cdot s/m^2}$),
- medium airflow resistivity ($r_s = 15\,000\,\mathrm{Pa\cdot s/m^2}$),
- high airflow resistivity ($r_s = 50\,000\,\mathrm{Pa\cdot s/m^2}$)

for two material thicknesses: 15 mm and 30 mm (Figs. 3a and 3b, respectively). For the covering material (thickness $D = 2.5$ mm), the analyses were performed with no distance behind the material and with a distance $L = 100$ mm behind the material (Figs. 3c and 3d, respectively).

The obtained results show the frequency ranges where the sound absorption coefficient is the most sensitive to changes in airflow resistivity. These results were used to formulate recommendations for the inverse method for determining airflow resistivity.

The analysis shows that the sensitivity index S_i of the sound absorption coefficient for porous materials changes with frequency and depends on the airflow resistivity r_s and the material thickness D (Figs. 3a, 3b). Sensitivity analysis has revealed that for materials with low airflow resistivity, the greatest sensitivity to changes in airflow resistivity occurs in the frequency range where the sound absorption coefficient increases from 0 to its maximum value. In contrast, for materials with high airflow resistivity, the range of greatest sensitivity shifts to the range where the absorption coefficient reaches its maximum. The value of airflow resistivity also determines the maximum value of the sound absorption coefficient and the frequency at which the maximum occurs. As a result, the value and frequency of the maximum absorption coefficient serve as key indicator for adjusting the sound absorption characteristics.

On the other hand, high negative values of the sensitivity index S_i can be observed in the low-frequency

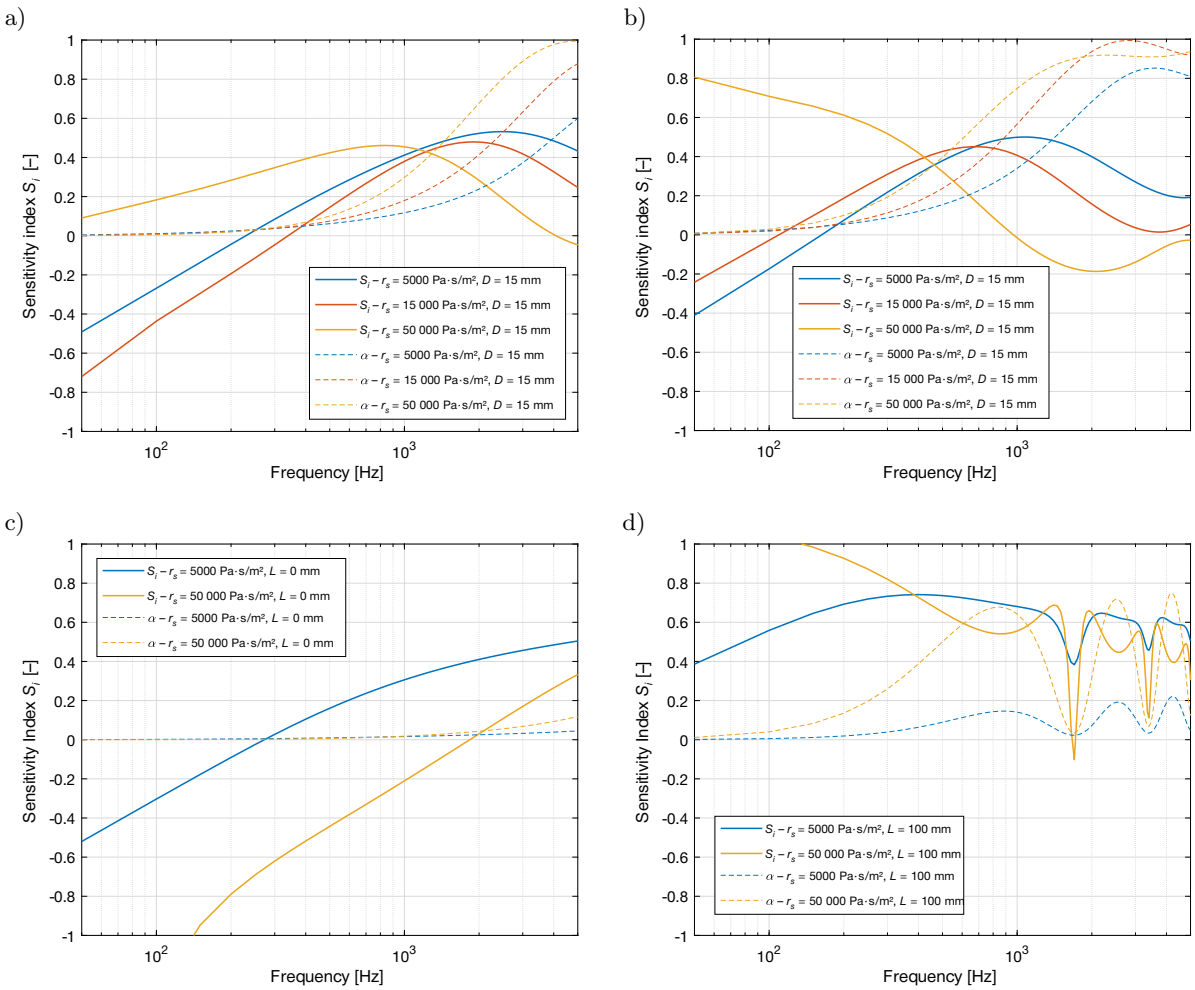

Fig. 3. Sensitivity indexes S_i of the sound absorption coefficient model to changes in airflow resistivity calculated for porous materials and covering materials across different airflow resistivity ranges. The results of calculations for porous material thicknesses: a) D = 15 mm, b) D = 30 mm; and for the covering material with thickness D = 2.5 mm: c) with no gap behind the material (L = 0 mm), d) with a gap (L = 100 mm).

range, indicating relatively large changes in the absorption coefficient. However, the absolute change in the absorption coefficient is small. Therefore, in this frequency range, the effect of changes in airflow resistivity is minimal, making it less significant when fitting the absorption characteristics to the measured values. To increase the accuracy of the inverse airflow resistivity determination, it is advantageous to fit the results over a frequency range that includes both the range in which the absorption coefficient increases and the region of the local maximum of the absorption coefficient.

In the case of thin materials and coverings that are directly backed by a rigid surface, the frequency at which the maximum occurs may be outside the measurement range (Figs. 3a, 3c). It is therefore advantageous to fit the sound absorption coefficient of a material sample placed over an air gap. The presence of an air gap behind the material has been shown to result in a shift of the sound absorption coefficient's maximums to lower frequencies (Fig. 3d). This effect serves to enhance the frequency range in which sensitivity is high, thereby facilitating improved matching across a broader frequency range.

3. Comparison of the methods

This section is concerned with a comparison of the two methods for determining airflow resistivity. The research was performed on seven different kinds of thick materials, which are primarily used as acoustic panel fillings, and two thin materials – polyester felts, which are mostly used as acoustic panel coverings or furniture upholstering (Fig. 4).

3.1. Covering materials

The airflow resistivity of thin materials was determined by employing both of the previously described methods. Measurements were taken for two different polyester felts, each with fibers of a different diameter and, presumably, different airflow resistivities. The

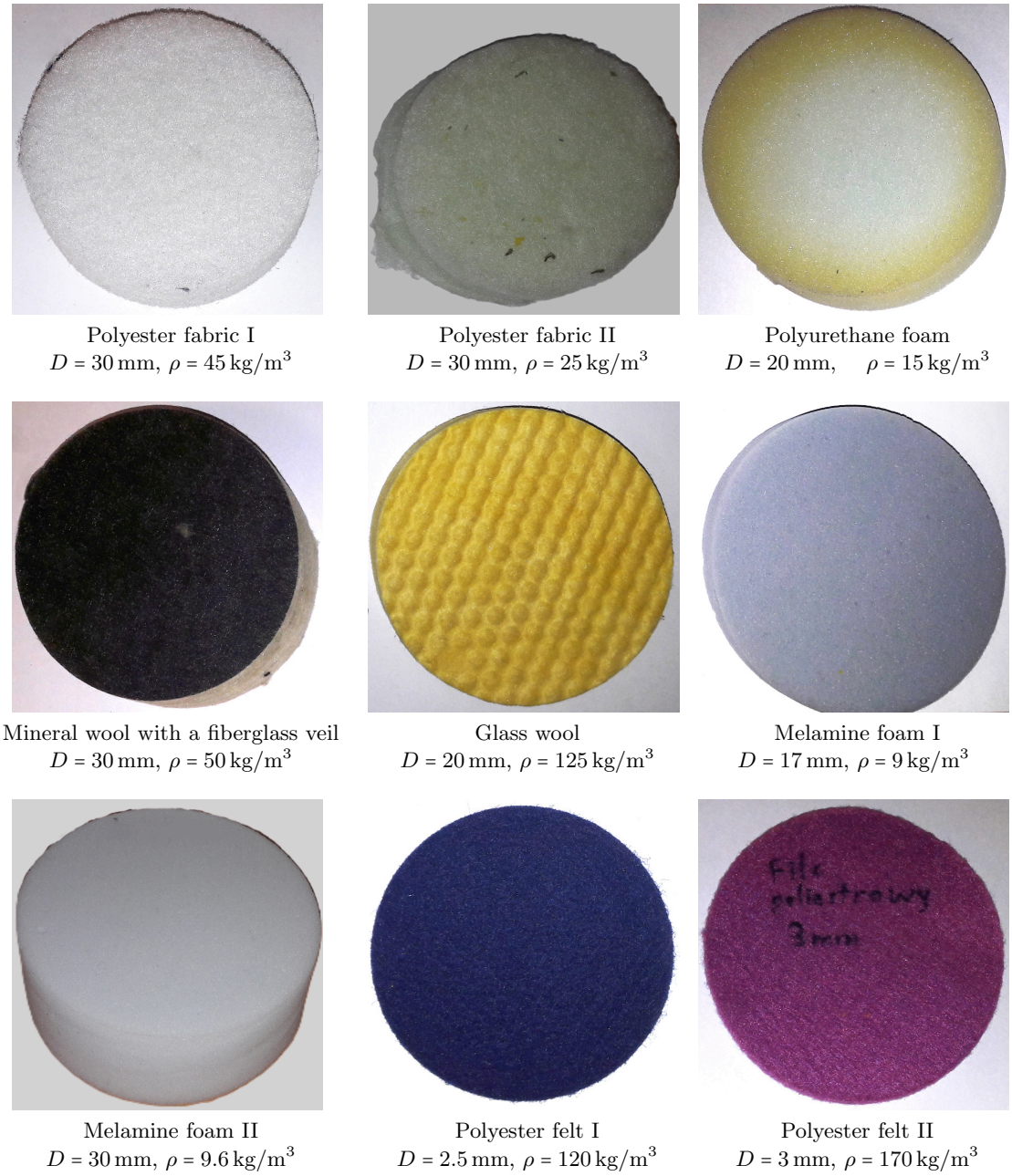

Fig. 4. Description of the measurement samples.

sound absorption coefficient was measured by placing the felts at the back of the impedance tube, with a distance ring to maintain the desired air gap L. The measurements of the sound absorption coefficient were performed for 10 different distances within the range L = 10 mm–200 mm (Fig. 5).

The matching was performed separately for three frequency ranges: f = 50 Hz–1600 Hz, which corresponds to measurements in the impedance tube of a large diameter (ø = 100 mm), f = 1600 Hz–6400 Hz (small impedance tube, ø = 29 mm), and for the wide frequency range f = 100 Hz–6400 Hz.

As the results show, increasing the air gap behind the sample L produces more local maxima associated with quarter-wavelength resonances (Fig. 5). In the inverse method, these maxima represent important points for obtaining more accurate matching. The choice of the frequency range for which the matching was performed is also important. The results from the large tube (Fig. 5a) include both the range in which the sound absorption coefficient increases and, depending on the distance L, also the local maxima. In contrast, the results from the small tube contain mainly local maxima, not always including the range in which the sound absorption coefficient increase starts from a minimum (Fig. 5b). Choosing a wide frequency range ensures that both the information about the sound absorption coefficient increase and the local maxima are

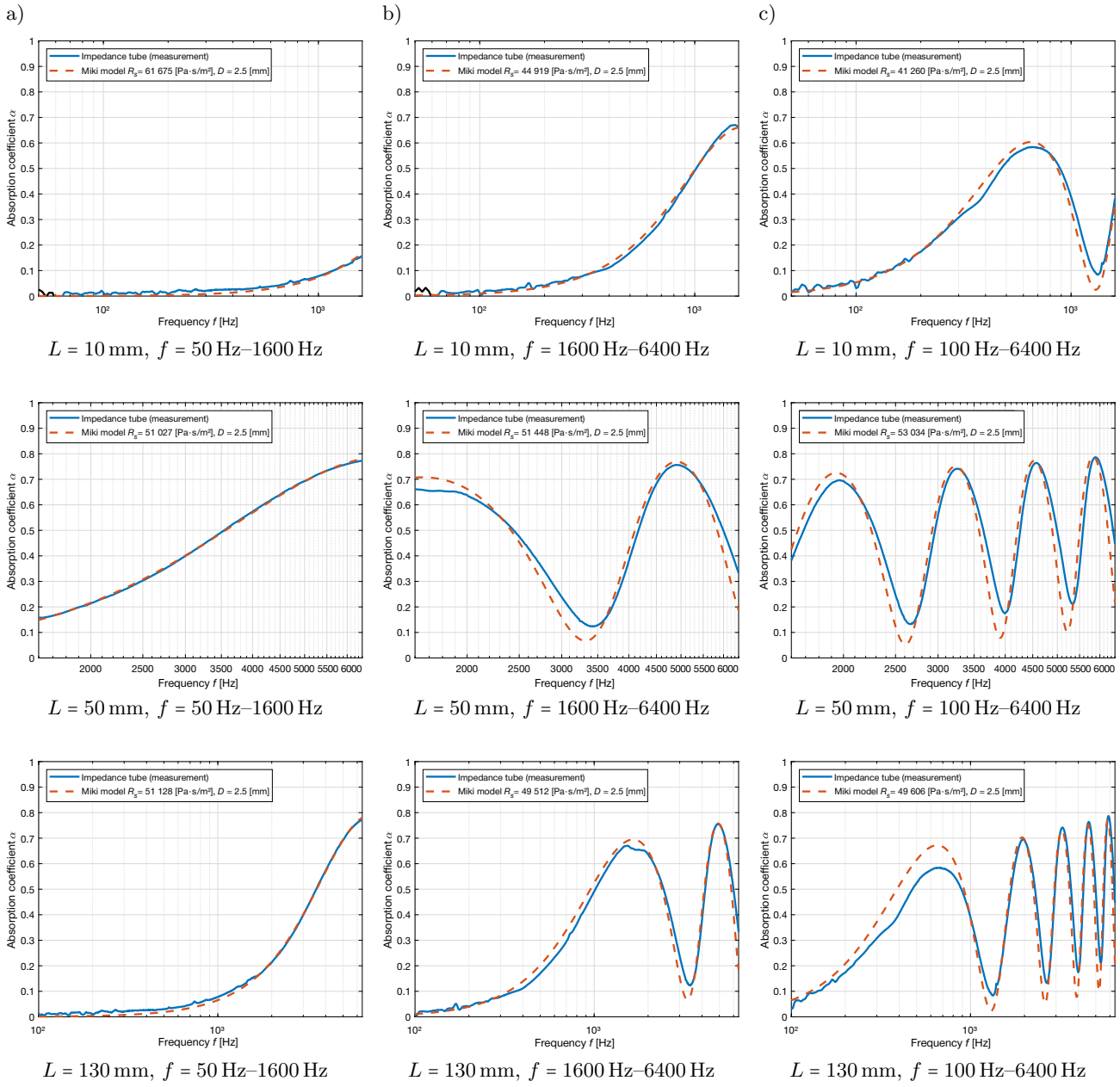

Fig. 5. Sound absorption coefficient of 2.5 mm-thick felt, where L is the air gap behind the specimen and f is frequency range: a) for large (ø = 100 mm) diameter tube, b) small (ø = 29 mm) diameter tube, c) for wide frequency range – combined results from both tubes.

acquired (Fig. 5c). As a result, the choice of the air gap behind the sample L and the frequency range translate into the value of airflow resistivity determined by matching the sound absorption coefficient.

The influence of the air layer L behind the material on the calculation of airflow resistivity using the inverse method is shown in Fig. 6.

The analysis showed that the 3 mm-thick felt with thinner fibers has significantly higher airflow resistivity. For the large tube, the results are mainly lower than those from the small tube. The results of the calculations performed for the wide frequency range are the average of the airflow resistivity obtained from both large and small tubes (Fig. 6). The obtained results of airflow resistivity differ most for air gaps of 10 mm and 50 mm for both felts. For the remaining air gaps, the results did not change significantly with the change of L. This confirms that the air gap improves the repeatability of the inverse method for determining airflow resistivity.

Table 1 compares the airflow resistivity values obtained with both methods. The results for the inverse method are the average values calculated for all the air gaps. A comparison of the determined airflow resistance values for both coverings reveals that the 2.5 mm-thick felt obtained values that are approx-

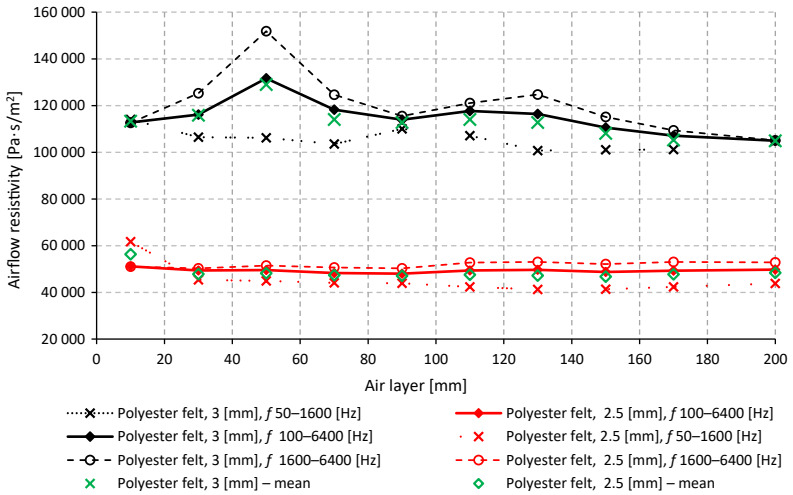

Fig. 6. Airflow resistivity of the porous materials, depending on the air gap behind the measurement sample and the frequency range (impedance tube measurement).

Table 1. Airflow resistivity of the covering under study.

No.	Material	Density ρ [kg/m^3]	Thickness D [mm]	r_s [Pa·s/m^2] (Inverse method)	r_s [Pa·s/m^2] (PLA – static airflow)
1	Polyester felt I	120	2.5	49 309	36 864
2	Polyester felt II	170	3	114 913	142 189

imately 25 % lower when measured using the PLA algorithm, while the 3 mm felt obtained values are 23 % higher for this method.

The comparison of sound absorption coefficients calculated using the airflow resistivities determined for both presented methods are shown in Fig. 7. The results of the sound absorption coefficients calculated and measured for the 3 mm-thick felt with a 70 mm air gap are in a good agreement for medium and high frequencies. Larger differences (though still not exceeding 0.1) can be observed at frequencies below 500 Hz. This means that the model is not very sensitive to changes in airflow resistivity and the value of sound absorption coefficient can be determined with reasonable accuracy.

3.2. Porous materials for filling acoustics panels

As demonstrated in Table 2, the values of airflow resistivities obtained by the inverse method and the

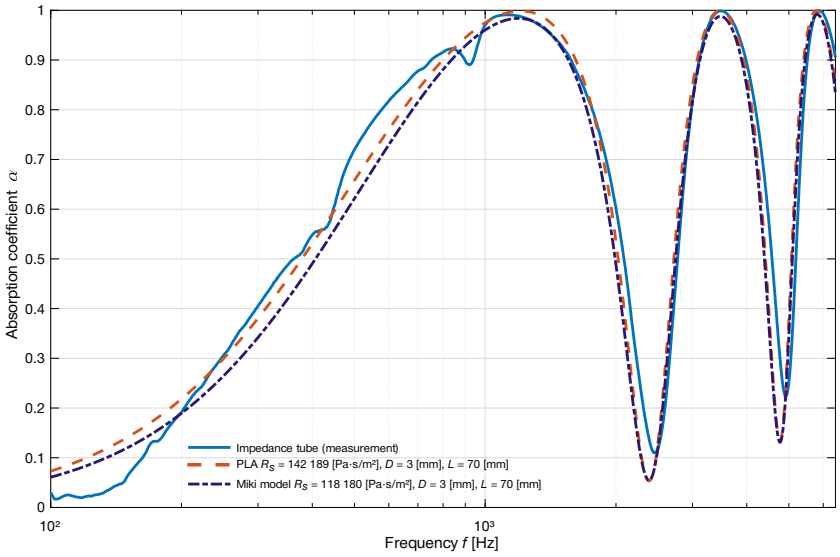

Fig. 7. Sound absorption coefficients measured and calculated based on the airflow resistivity determined with the inverse method and airflow resistivity measurement (PLA algorithm) for a 3 mm-thick polyester felt mounted at a 70 mm air gap.

Table 2. Airflow resistivity of materials used for filling the acoustic panels.

No.	Material	Density ρ [kg/m^3]	Thickness D [mm]	R^2	r_s [Pa·s/m^2] (Inverse method)	r_s [Pa·s/m^2] (PLA – static airflow)	Relative error d [%]
1	Polyester fabric I	45	30	0.993	2436	2435	0.04
2	Polyester fabric II	25	30	0.973	5024	4840	3.80
3	Mineral wool with fiberglass veil	50	30	0.983	16 474	18 603	11.44
4	Glass wool	125	20	0.960	102 893	126 154	18.44
5	Polyurethane foam (CME = CV)	15	20	0.965	5099	5040	1.17
6	Melamine foam I	9	17	0.995	6941	7922	12.38
7	Melamine foam II	9.6	30	0.988	8701	8652	0.57

static airflow measurement method (PLA algorithm) for a wide frequency range are shown. In order to evaluate the results, the relative error between the values obtained from the two methods was determined. This was done by using the following equation:

$$\delta = \frac{|r_{s1} - r_{s2}|}{r_{s1}}, \tag{17}$$

where r_{s1} is the airflow resistivity from the inverse method and r_{s2} is the value obtained from modified static airflow measurements. It is acknowledged that the true value of airflow resistivity is unknown, so the relative error serves a comparison between the two different measurement techniques. The analysis of airflow resistivity shows that for materials with low airflow resistivity (up to around 10 000 Pa·s/m^2), the dif-

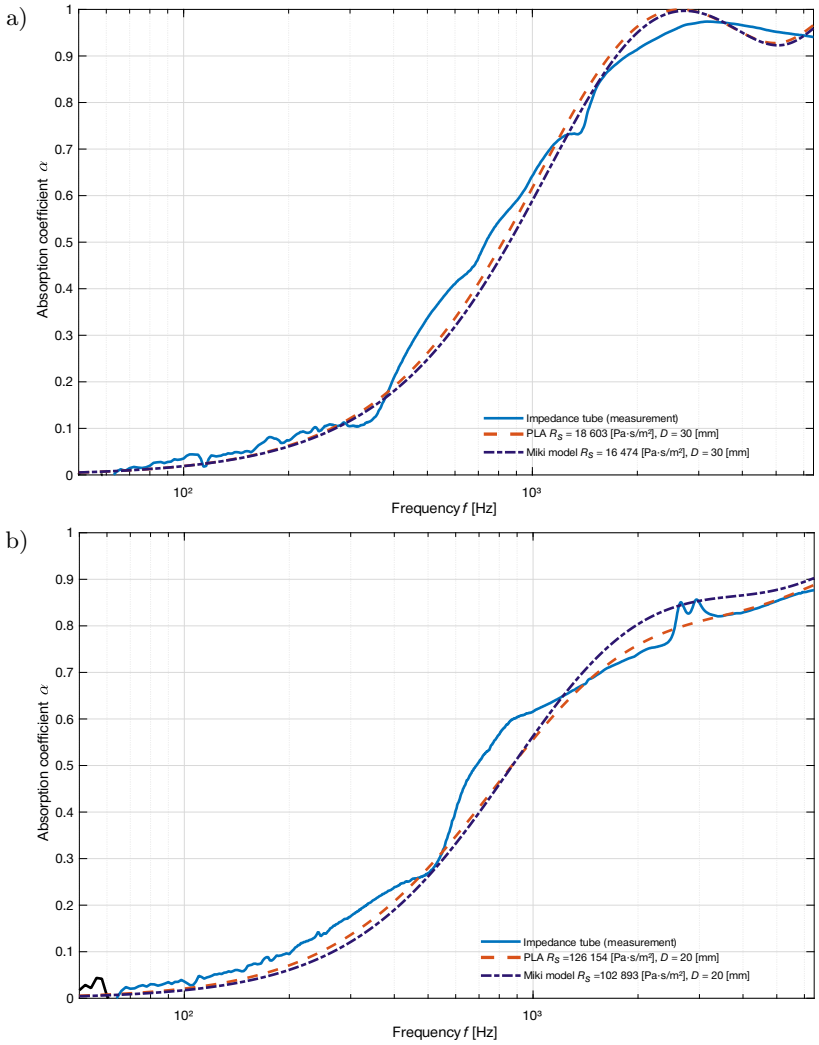

Fig. 8. Sound absorption coefficient: measured and calculated based on the airflow resistivity determined with the inverse method and with the airflow resistivity measurement method (PLA algorithm) for: a) mineral wool, b) glass wool.

ferences in the determined values of airflow resistivity do not exceed 12 %. However, as the airflow resistivity values increase, the discrepancy between the values obtained by the two methods also increases, reaching up to 18 % for glass wool.

However, the comparison of the sound absorption coefficient values determined and measured for mineral wool and glass wool shows good agreement (Fig. 8).

The largest differences between the determined values do not exceed 0.1 and can be observed at high frequencies. Mineral wool demonstrates a better match compared to glass wool, particularly in the range where the absorption coefficient is increasing (Fig. 8a). To improve the fitting of the curves, a different model specifically developed for glass wools could be used (Fig. 8b). Similarly to the covering materials, the calculation model is not very sensitive to changes in airflow resistivity, and even for large changes in airflow resistivity, the values of the sound absorption coefficient can be determined with good accuracy.

4. Discussion

The findings of the research indicate that both methodologies employed for the estimation of the airflow resistivity of porous materials, with densities ranging from 9.6 kg/m^3 to 45 kg/m^3, facilitate the precise calculation of the sound absorption coefficient. However, a higher discrepancy is observed in the estimation of airflow resistivity for materials characterized by high density and high airflow resistivity (Table 2).

The discrepancy between the methods may be attributed to the selection of the computational model for the inverse method. Empirical models are fitted to specific data sets, thus constraining their ability to predict the behavior of materials with significantly different properties or under conditions significantly different from those under which measurements were made (Komatsu, 2008). Consequently, these models may be less accurate in predicting acoustic properties across a broader range of material parameters, such as density or flow resistance. The accuracy of the inverse method is contingent on the execution of the fitting procedure within the applicable range of the relevant approximations (Bonfiglio, Pompoli, 2013). Conversely, the outcomes derived from the inverse method are also directly influenced by the quality of the experimental data, such as the sound absorption coefficient. Errors in the input data can propagate to the inversion results (Pelegrinis *et al.*, 2016).

The complexity and imprecision inherent in the determination of the physical parameters of porous materials constitute a substantial challenge, especially for more complicated models (Bonfiglio, Pompoli, 2013). Consequently, the present study opted for a more straightforward model that necessitates only flow resistivity for the inversion method.

The flow resistivity measurement method under discussion is subject to factors that can influence measurement error, with one potential source of error being the leakage of air through the side of the material sample mounted in the holder during the airflow method. Other issues arise from non-linearities in the relationship between airflow resistance R_s and airflow velocity u (Melnyk *et al.*, 2018).

However, it is worthwhile to analyze the significance of the observed discrepancies and their impact on the prediction of sound absorption coefficients. The findings for both upholstery and thicker porous materials demonstrate that the discrepancies in the determined airflow resistivity values for low-density materials (up to $\rho < 50\,\mathrm{kg/m^3}$) and low-resistivity airflows (up to $r_s < 30\,000\,\mathrm{Pa\cdot s/m^2}$) do not exceed 15 % between the methods. For materials with higher densities and flow resistivities, the differences can reach up to 18 %. Nevertheless, a comparison of sound absorption coefficients calculated from airflow resistivity values obtained by both methods with values measured in the impedance tube revealed that these differences do not significantly affect the sound absorption coefficient values. According to these results, the process of determining airflow resistivity can be simplified by using the inverse method for measurement samples with a diameter of 100 mm only. The study also investigated the impact of the method used to mount thin and covering materials on the accuracy of determining airflow resistivity using the inverse method. It was found that mounting the material with an air gap is necessary for obtaining accurate results, and that for achieving repeatable results, a minimum distance of 70 mm is required.

5. Conclusions

In the present study, two methods for determining the airflow resistivity of porous materials were compared and validated. The first method was a modified version of the standardized method based on static airflow, as proposed by Melnyk *et al.* (2018). In this method, a linear approximation was used to improve the fit between the measured airflow resistivity and sound absorption coefficient results. The second method, known as the inverse method, involved matching the theoretical sound absorption coefficient with the impedance tube measurement results. The primary objective of the research was to evaluate the accuracy of airflow resistivity measurement for certain materials and to assess the effect of this parameter on the agreement between the predicted sound absorption coefficient and the impedance tube measurement results.

The study was carried out on different types of porous materials with thicknesses ranging from 2.5 mm to 30 mm and densities from 9 kg/m^3 to 170 kg/m^3.

Thin covering materials, used for upholstery, were investigated as well as thicker porous materials typically used in acoustic panels or as furniture infill. The selection of materials for testing was based on their different airflow resistivities.

The results of the research suggest that for porous materials up to approximately 30-mm thick, variations in measured airflow resistivity values do not have a significant effect on the sound absorption coefficient. Consequently, both methods can be used to determine the airflow resistivity required to calculate the sound absorption coefficient of porous materials and layered structures, including upholstery, without the need for repeated measurements of specific configurations. This will greatly speed up the process of selecting materials and upholstery for specific acoustic purposes.

Fundings

This research did not receive any specific grant from funding agencies in the public, commercial, or not-for-profit sectors.

Conflict of interest

The authors declare that they have no known competing financial interests or personal relationships that could have appeared to influence the work reported in this paper.

Authors' contributions

Mykhaylo Melnyk – conceptualization, development of a PLA method, measurement and data analysis, writing the manuscript; Jarosław Rubacha – conceptualization, development of a invers method, data analysis, writing the manuscript; Artur Flach – measurement and data analysis, verification of measurement, manuscript review; Aleksandra Chojak – measurement and data analysis, writing the manuscript; Tadeusz Kamisiński – supervision, results analysis, manuscript review; Wojciech Zabierowski – supervision, manuscript review; Marek Iwaniec – supervision, manuscript review; Andriy Kernytskyy – manuscript review.

References

1. Allard J.F., Atalla N. (2009), *Propagation of Sound in Porous Media: Modelling Sound Absorbing Materials*, Wiley, https://doi.org/10.1002/9780470747339.
2. Allard J.-F., Champoux Y. (1992), New empirical equations for sound propagation in rigid frame fibrous materials, *The Journal of the Acoustical Society of America*, **91**(6): 3346–3353, https://doi.org/10.1121/1.402824.
3. ASTM C522-03 (2022), *Standard test method for airflow resistance of acoustical materials*, ATM International.
4. Bonfiglio P., Pompoli F. (2013), Inversion problems for determining physical parameters of porous materials: Overview and comparison between different methods, *Acta Acustica United with Acustica*, **99**(3): 341–351, https://doi.org/10.3813/AAA.918616.
5. Cao L., Fu Q., Si Y., Ding B., Yu J. (2018), Porous materials for sound absorption, *Composites Communications*, **10**: 25–35, https://doi.org/10.1016/j.coco.2018.05.001.
6. Cox T., D'Antonio P. (2016), *Acoustic Absorbers and Diffusers. Theory, Design and Application*, 3rd ed., CRC Press, https://doi.org/10.1201/9781315369211.
7. Crocker M.J. [Ed.] (2007), *Handbook of Noise and Vibration Control*, Wiley, https://doi.org/10.1002/9780470209707.
8. Cuenca J., Göransson P., De Ryck L., Lähivaara T. (2022), Deterministic and statistical methods for the characterisation of poroelastic media from multi-observation sound absorption measurements, *Mechanical Systems and Signal Processing*, **163**: 108186, https://doi.org/10.1016/j.ymssp.2021.108186.
9. Delany M.E., Bazley E.N. (1970), Acoustical properties of fibrous absorbent materials, *Applied Acoustics*, **3**(2): 105–116, https://doi.org/10.1016/0003-682X(70)90031-9.
10. Dell A., Krynkin A., Horoshenkov K.V. (2021), The use of the transfer matrix method to predict the effective fluid properties of acoustical systems, *Applied Acoustics*, **182**: 108259, https://doi.org/10.1016/j.apacoust.2021.108259.
11. Doutres O., Salissou Y., Atalla N., Panneton R. (2010), Evaluation of the acoustic and non-acoustic properties of sound absorbing materials using a three-microphone impedance tube, *Applied Acoustics*, **71**(6): 506–509, https://doi.org/10.1016/j.apacoust.2010.01.007.
12. Gibson L.J., Ashby M.F. (1997), *Cellular Solids: Structure and Properties*, 2nd ed., Cambridge University Press, https://doi.org/10.1017/CBO9781139878326.
13. Herrero-Durá I., Cebrecos Ruíz A., García-Raffi L.M., Romero-García V. (2019), Matrix formulation in acoustics: The transfer matrix method [in Spanish: Formulación matricial en Acústica: El método de la matriz de transferencia], *Modelling in Science Education and Learning*, **12**(2): 153, https://doi.org/10.4995/msel.2019.12148.
14. Hou X., Du S., Liu Z., Guo J., Li Z. (2017), A transfer matrix approach for structural – Acoustic correspondence analysis of diesel particulate filter, *Advances in Mechanical Engineering*, **9**(9), https://doi.org/10.1177/1687814017722495.
15. Huang S., Li Y., Zhu J., Tsai D.P. (2023), Sound-absorbing materials, *Physical Review Applied*, **20**(1): 010501, https://doi.org/10.1103/PhysRevApplied.20.010501.

16. International Organization for Standardization (1996), *Acoustics – Determination of sound absorption coefficient and impedance in impedance tubes. Part 1: Method using standing wave ratio* (ISO Standard No. 10534-1:1996), https://www.iso.org/standard/18603.html.

17. International Organization for Standardization (2003), *Acoustics – Measurement of sound absorption in a reverberation room* (ISO Standard No. 354:2003), https://www.iso.org/standard/34545.html.

18. International Organization for Standardization (2018), *Acoustics – Determination of airflow resistance. Part 1: Static airflow method* (ISO Standard No. 9053-1:2018), https://www.iso.org/standard/69869.html.

19. International Organization for Standardization (2023), *Acoustics – Determination of sound absorption coefficient and impedance in impedance tubes. Part 2: Two-microphone technique for normal sound absorption coefficient and normal surface impedance* (ISO Standard No. 10534-2:2023, https://www.iso.org/standard/81294.html.

20. Jeong C.-H. (2020), Flow resistivity estimation from practical absorption coefficients of fibrous absorbers, *Applied Acoustics*, **158**: 107014, https://doi.org/10.1016/j.apacoust.2019.107014.

21. Johnson D.L., Koplik J., Dashen R. (1987), Theory of dynamic permeability and tortuosity in fluid-saturated porous media, *Journal of Fluid Mechanics,* **176**(1): 379–402, https://doi.org/10.1017/S0022112087000727.

22. Kamisiński T., Brawata K., Pilch A., Rubacha J., Zastawnik M. (2012), Sound diffusers with fabric covering, *Archives of Acoustics*, **37**(3): 317–322, https://doi.org/10.2478/v10168-012-0040-5.

23. Komatsu T. (2008), Improvement of the Delany–Bazley and Miki models for fibrous sound-absorbing materials, *Acoustical Science and Technology*, **29**(2): 121–129, https://doi.org/10.1250/ast.29.121.

24. Lafarge D., Lemarinier P., Allard J.F., Tarnow V. (1997), Dynamic compressibility of air in porous structures at audible frequencies, *The Journal of the Acoustical Society of America*, **102**(4): 1995–2006, https://doi.org/10.1121/1.419690.

25. Melnyk M., Rubacha J., Kamisiński T., Majchrzak A. (2018), Application of MEMS sensors for the automation of a laboratory stand for the measurement of the flow resistance of porous materials, [in:] *2018 XIV-th International Conference on Perspective Technologies and Methods in MEMS Design (MEMSTECH)*, pp. 28–34, https://doi.org/10.1109/MEMSTECH.2018.8365695.

26. Miki Y. (1990), Acoustical properties of porous materials. Modifications of Delany–Bazley models, *Journal of the Acoustical Society of Japan (E)*, **11**(1): 19–24, https://doi.org/10.1250/ast.11.19.

27. Müller-Giebeler M., Berzborn M., Vorländer M. (2024), Free-field method for inverse characterization of finite porous acoustic materials using feed forward neural networks, *The Journal of the Acoustical Society of America*, **155**(6): 3900–3914, https://doi.org/10.1121/10.0026239.

28. Oliva D., Hongisto V. (2013), Sound absorption of porous materials – Accuracy of prediction methods, *Applied Acoustics*, **74**(12): 1473–1479, https://doi.org/10.1016/j.apacoust.2013.06.004.

29. Pelegrinis M.T., Horoshenkov K.V., Burnett A. (2016), An application of Kozeny–Carman flow resistivity model to predict the acoustical properties of polyester fibre, *Applied Acoustics*, **101**: 1–4, https://doi.org/ 10.1016/j.apacoust.2015.07.019.

30. Rubacha J., Pilch A., Zastawnik M. (2012), Measurements of the sound absorption coefficient of auditorium seats for various geometries of the samples, *Archives of Acoustics*, **37**(4): 483–488, https://doi.org/10.2478/v10168-012-0060-1.

31. Saltelli A., Tarantola S., Campolongo F., Ratto M. (2004), *Sensitivity Analysis in Practice: A Guide to Assessing Scientific Models*, Wiley.

32. Sebaa N., Fellah Z.E.A., Fellah M., Lauriks W., Depollier C. (2005), Measuring flow resistivity of porous material via acoustic reflected waves, *Journal of Applied Physics*, **98**(8): 084901, https://doi.org/10.1063/1.2099510.

33. Tao Y., Ren M., Zhang H., Peijs T. (2021), Recent progress in acoustic materials and noise control strategies – A review, *Applied Materials Today*, **24**: 101141, https://doi.org/10.1016/j.apmt.2021.101141.

34. Vorländer M. (2008), *Auralization. Fundamentals of Acoustics, Modelling, Simulation, Algorithms and Acoustic Virtual Reality*, Springer Berlin, Heidelberg, https://doi.org/10.1007/978-3-540-48830-9.

35. Zea E., Brandão E., Nolan M., Cuenca J., Andén J., Svensson U.P. (2023), Sound absorption estimation of finite porous samples with deep residual learning, *The Journal of the Acoustical Society of America*, **154**(4): 2321–2332, https://doi.org/10.1121/10.0021333.

36. Zhao X.-D., Yu Y.-J., Wu Y.-J. (2016), Improving low-frequency sound absorption of micro-perforated panel absorbers by using mechanical impedance plate combined with Helmholtz resonators, *Applied Acoustics*, **114**: 92–98, https://doi.org/10.1016/j.apacoust.2016.07.013.